Osteoporosis International (2019) 30:1099–1110
https://doi.org/10.1007/s00198-019-04894-y

ORIGINAL ARTICLE

Discrimination of osteoporosis-related vertebral fractures by DXA-derived 3D measurements: a retrospective case-control study

M. López Picazo[1,2] · L. Humbert[1] · S. Di Gregorio[3] · M. A. González Ballester[2,4] · L.M. del Río Barquero[3]

Received: 7 September 2018 / Accepted: 8 February 2019 / Published online: 15 February 2019

Abstract

Summary A retrospective case-control study assessing the association of DXA-derived 3D measurements with osteoporosis-related vertebral fractures was performed. Trabecular volumetric bone mineral density was the measurement that best discriminates between fracture and control groups.

Introduction The aim of the present study was to evaluate the association of DXA-derived 3D measurements at the lumbar spine with osteoporosis-related vertebral fractures.

Methods We retrospectively analyzed a database of 74 postmenopausal women: 37 subjects with incident vertebral fractures and 37 age-matched controls without any type of fracture. DXA scans at the lumbar spine were acquired at baseline (i.e., before the fracture event for subjects in the fracture group), and areal bone mineral density (aBMD) was measured. DXA-derived 3D measurements, such as volumetric BMD (vBMD), were assessed using a DXA-based 3D modeling software (3D-SHAPER). vBMD was computed at the trabecular, cortical, and integral bone. Cortical thickness and cortical surface BMD were also measured. Differences in DXA-derived measurements between fracture and control groups were evaluated using unpaired *t* test. Odds ratio (OR) and area under the receiver operating curve (AUC) were also computed. Subgroup analyses according to fractured vertebra were performed.

Results aBMD of fracture group was 9.3% lower compared with control group ($p < 0.01$); a higher difference was found for trabecular vBMD in the vertebral body (− 16.1%, $p < 0.001$). Trabecular vBMD was the measurement that best discriminates between fracture and control groups, with an AUC of 0.733, against 0.682 for aBMD. Overall, similar findings were observed within the subgroup analyses. The L1 vertebral fractures subgroup had the highest AUC at trabecular vBMD (0.827), against aBMD (0.758).

Conclusion This study showed the ability of cortical and trabecular measurements from DXA-derived 3D models to discriminate between fracture and control groups. Large cohorts need to be analyzed to determine if these measurements could improve fracture risk prediction in clinical practice.

Keywords 3D modeling · Fracture risk · Osteoporosis · Trabecular bone · Vertebral fracture · Volumetric bone mineral density

Introduction

The absence of symptoms in the early stage of the osteoporosis disease leads to millions of people remaining undiagnosed and untreated, increasing their probabilities to suffer from a fracture. Worldwide, 8.9 million of osteoporosis-related or fragility fractures occur each year, resulting in a fracture every 3 s [1]. Vertebral fractures, the most common osteoporosis-related fracture [2], occur after low impact trauma or by compression slowly over time [3]. These fractures are associated with chronic back pain, spinal deformity, limited physical functioning, and an increased risk of hospitalization and mortality [4], although they can also be asymptomatic. It is estimated that only one-third of vertebral fractures get clinical attention [3].

Dual-energy X-ray absorptiometry (DXA) is the standard exam for osteoporosis diagnosis and fracture risk [5, 6], as it is a low-radiation and non-expensive technique. DXA provides

✉ M. López Picazo
mirella.lopez.picazo@gmail.com

1 Musculoskeletal Unit, Galgo Medical, Barcelona, Spain

2 BCN Medtech, Universitat Pompeu Fabra, Barcelona, Spain

3 CETIR Grup Mèdic, Barcelona, Spain

4 ICREA, Barcelona, Spain

2D images in which the areal bone mineral density (aBMD) projected along the anteroposterior (AP) direction is measured. Low aBMD measured at AP DXA scans is among the strongest fracture risks [5–7]. A standard deviation decrease in aBMD leads to a 1.5- to 3.0-fold increased risk of fracture depending on site-specific measurement and fracture site [7]. However, a low aBMD is not enough to explain all fractures. State-of-the-art studies suggested that the risk of fracture is very high when a low aBMD is present, but by no means negligible when it is normal [5–10]. Therefore, aBMD for fracture risk prediction has low sensitivity (detection rate) at acceptable specificity [9].

The majority of osteoporosis-related vertebral fractures are located in the vertebral body [11]. In spine AP DXA images, the vertebral body superimposes with the posterior vertebral elements, therefore the BMD in the vertebral body cannot be estimated separately. Fracture risk also depends on bone quality. Trabecular bone architecture and cortical bone thickness are important elements that determine bone quality [12]. However, trabecular and cortical bone compartments are difficult to assess separately in AP DXA scans.

As an alternative to DXA, quantitative computed tomography (QCT) provides a 3D analysis of bone structures. Volumetric BMD (vBMD) in the vertebral body can be measured independently of the posterior vertebral elements, and even trabecular and cortical structures can be evaluated [5, 13, 14]. The association of QCT-derived vBMD with vertebral fracture has been studied previously [10, 15–19]. QCT-based finite element analysis is also used to know the mechanical properties of the vertebrae and predict vertebral fracture risk [19–22]. However, QCT results in exposure to a higher dose of radiation and is more expensive, compared with DXA. Consequently, QCT is rarely used in clinical practice for fracture risk evaluation.

To overcome the limitations of DXA and QCT, 3D modeling methods were proposed to estimate the 3D shape and density distribution of bones from a limited number of DXA scans [23–27]. Those approaches use a statistical 3D shape and density model of the bone, built from a training set of QCT scans, which is registered onto the DXA scans to obtain the 3D subject-specific QCT-like model of the bone. Whitmarsh et al. [26] obtain 3D subject-specific estimates of the lumbar spine (from L2 to L4) by registering a statistical model onto two DXA images (AP and lateral views). Although they performed measurements in the trabecular compartment, no specific algorithm is proposed to quantify the cortical bone. In a previous study [27], we proposed a similar method to estimate the 3D shape and vBMD at the lumbar spine (from vertebra L1 to L4) but using a single AP DXA image. This method also performs a separate assessment of the cortical and the trabecular compartments, giving special emphasis to the vertebral body. Accuracy of those methods [23–27] was evaluated by comparing DXA- and QCT-derived 3D models and measurements. However, to the best of our knowledge, no study has reported on the association of output measurements provided by DXA-based 3D modeling techniques with vertebral fracture.

This paper presents a retrospective case-control study including postmenopausal Caucasian women who experienced a vertebral fracture event and age-matched controls. DXA-derived 3D measurements were obtained at baseline (at least 1 year before the vertebral fracture event for subjects in the fracture group) for each subject using lumbar spine AP DXA scans and a DXA-based 3D modeling technique [27]. The ability of DXA-derived 3D measurements to discriminate between fracture and control groups was assessed. As the fracture group included various types of vertebral fractures, subgroup analyses were performed to analyze the difference between groups depending on the type of fracture.

Materials and methods

Study population

We retrospectively analyzed a database collected at CETIR Grup Mèdic (Barcelona, Spain). The database is composed of postmenopausal Caucasian women over 40 years old with baseline and follow-up visits, both performed between the years 2000 and 2010. Subjects of the database were stratified in two groups: patients with incident vertebral fractures related to osteoporosis (fracture group) and age-matched subjects without any type of fracture (control group). Inclusion criteria for the fracture group were no prior osteoporotic fractures in any skeletal site at baseline visit (i.e., no prevalent fractures at baseline), incident vertebral fracture(s) related to osteoporosis at follow-up visit between 1 and 10 years from baseline, and no incident osteoporotic fractures in any skeletal site other than spine during the follow-up period. Conversely, inclusion criteria for the control group were no prior osteoporotic fractures in any skeletal site at baseline and during at least 7 years from baseline visit (i.e., no prevalent fractures at baseline and no incident fractures at follow-up visit). Individuals in both groups were excluded if they had skeletal disease other than osteoporosis, such as severe osteoarthritis, severe scoliosis, spondylitis, spinal infection, or abnormal bone growth, or undergone spinal surgery. Vertebrae affected by mild local structural changes were not used as exclusion criteria for the subject, neither to discard vertebrae for the analysis. Each subject of the fracture group was age-matched (± 5 years) with a subject of the control group. Clinical parameters such as age, weight, height, and BMI were collected for each subject at baseline.

Vertebral fractures were confirmed by a radiologist specialist using vertebral fracture assessment (VFA), in accordance with semi-quantitative Genant classification criteria [11]. The

absence of fracture was determined by revising the clinical history of the subjects, by analyzing the AP DXA scans at baseline and follow-up visits, and by discarding any subjects showing a height decrease of 2 cm or more between baseline and follow-up visit.

Three subgroups were identified in the fracture group depending on the type of fracture. The first subgroup was composed by the subjects that had at least one lumbar vertebra fractured. The second subgroup was composed by the subjects that had at least the vertebra L1 fractured. The third subgroup was composed of the subjects that had at least one thoracic vertebra fractured. Subjects from each subgroup may have, in addition to the type of fracture befitting with its group, other types of vertebral fractures.

This study was conducted as prescribed by the latest version of the Declaration of Helsinki. Ethical approval was given by the CETIR Grup Mèdic scientific committee for the use of retrospective clinical data and of results of bone measurements in the scope of this study. Each subject was ensured of anonymity which was maintained by using subject-specific numeric codes on all records.

Medical images and DXA-derived 2D measurements

A lumbar spine AP DXA scan was acquired at baseline for all subjects included in the study. DXA scans were performed using a Prodigy densitometer (GE Healthcare, Madison, WI, USA) and analyzed using enCORE software (v14.10, GE Healthcare, Madison, WI, USA). DXA scans and analyses were performed by a trained radiologist at CETIR Grup Mèdic according to the manufacturer's recommendations. DXA-derived 2D measurements, such as aBMD (in g/cm^2), bone mineral content (BMC, in g), and area (in cm^2), were measured in the spine AP DXA scans at vertebrae L1 to L4 (L1–L4 segment). T-scores were evaluated using GE Lunar normative data for Spain.

DXA-derived 3D measurements

DXA-derived 3D measurements at L1–L4 segment were obtained using the software 3D-SHAPER (Galgo Medical, Barcelona, Spain) and the AP DXA scans acquired at baseline (before the fracture). 3D-SHAPER computes a 3D subject-specific shape and density model of the lumbar spine from a single AP DXA image, as described in [27] and briefly summarized thereafter. First, the 3D subject-specific estimation is obtained by registering and fitting a statistical shape and density model onto the AP DXA image. The statistical model was previously generated using a training database of QCT scans from Caucasian men and women. Then, the periosteal and endocortical surfaces of the cortical layer are searched by using a model-based algorithm [27, 28]. The algorithm computes the density profile along the normal vector at each node of the 3D surface mesh and fit to a function of the cortical thickness and density, the location of the cortex, the density of surrounding tissues, and the imaging blur. Finally, DXA-derived 3D measurements are performed at different vertebral regions and bone compartments. vBMD (in mg/cm^3), BMC (in g), and volume (in cm^3) were measured at the integral bone of the total vertebra and the vertebral body. These measurements were also obtained for the trabecular and cortical compartments at the vertebral body. The mean cortical thickness (Cort. Th., in mm) and the cortical surface BMD (cortical sBMD, in mg/cm^2) were measured at the vertebral body. The cortical sBMD is the amount of cortical bone per unit area integrated along the normal vector at each node of the 3D vertebral body surface mesh. It was computed as the multiplication of the cortical vBMD (in mg/cm^3) and the Cort. Th. (in cm).

Statistical analysis

Descriptive statistics, including means and standard deviations (SD), were used to analyze the fracture and control groups. Differences between groups at baseline were assessed using the parametric Student's t test, after checking for normality. A p value < 0.05 was considered statistically significant. Univariate logistic regressions (backward) were used to investigate possible correlations between independent variables (weight, height, BMI, and DXA-derived 2D and 3D measurements) and the status of the fracture. The ability of DXA-derived measurements to discriminate between fracture and control subjects was evaluated by using the area under the receiver operating characteristic curve (AUC). Odds ratio (OR) with 95% confidence intervals (CI) was calculated to estimate the odds of a vertebral fracture occurring for every 1 SD change in the DXA-derived measurements. To visualize the differences between groups in vBMD distribution, the mean 3D shape and density were computed for each group. Slices in the mid vertebral body plane were used to visualize the anatomical distribution of differences in vBMD. Cortical sBMD distribution was also computed for each group. Differences in cortical sBMD distribution were displayed onto the average shape instance. The statistical analysis was performed for the whole database and for each subgroup separately. Statistical analyses were conducted using MATLAB Academic (release R2015b, MathWorks, Inc., Natick, Massachusetts, United States).

Results

Subject's characteristic

Seventy-four postmenopausal Caucasian women were included in this study: 37 patients with osteoporosis-related vertebral

fractures (fracture group) and 37 age-matched subjects without any type of fracture (control group). No significant differences (p value ≥ 0.05) were observed in terms of age, weight, height, and BMI between fracture and control groups (Table 1). Patients in the fracture group had a vertebral fracture event on average (± SD) at 3.2 ± 2.4 years from baseline. Absence of osteoporotic fracture event was ensured for controls over an average period of 9.0 ± 1.6 years.

The fracture group was composed of 30 patients with a single vertebral fracture and 7 with multiple vertebral fractures. A total of 48 incident vertebral fractures were found in the 37 patients of the fracture group: 2 T4, 2 T7, 1 T8, 1 T9, 3 T10, 1 T11, 9 T12, 15 L1, 6 L2, 4 L3, and 4 L4. The information of whether the patient in the fracture group had wedge, biconcave, or crush deformity was not available for all the subjects. The grade of the fracture was classified as severe in 28 patients.

DXA-derived 2D measurements

Based on the WHO classification criteria, 97% of the patients in the fracture group and 84% of the subjects in the control group had a low aBMD (L1–L4 T-score < − 1). The vertebral fracture group was composed by 29 women with osteoporosis, 7 with low bone mass, and 1 with normal bone mass, whereas the control group was composed by 14 women with osteoporosis, 17 with low bone mass, and 6 with normal bone mass.

Mean aBMD at L1–L4 segment of vertebral fracture group (whole database) was 9.3% lower compared with control group ($p < 0.01$, Table 2). No significant differences were observed in BMC and area. aBMD can discriminate between fracture group and controls with an AUC = 0.682. Each incremental decrease of 1 SD in aBMD was associated with an increase of twice of the odds of presenting a vertebral fracture (OR 2.033 95% CI [1.202–3.438]).

DXA-derived 3D measurements

Integral vBMD at the total vertebra of the fracture group was 10.2% lower compared with control group ($p < 0.01$), (whole database, Table 2). At the vertebral body, differences in vBMD were more pronounced in the trabecular bone (− 16.1%, $p < 0.001$) than in the integral bone (− 11.3%,

Table 1 Characteristics at baseline of the subjects included in fracture and control groups according to fracture site

	Control	Fracture	p*
Vertebral fracture (whole database)			
Number	37	37	
Age (years)	65.3 ± 8.1 [50.0–79.7]	65.5 ± 7.6 [48.8–78.2]	0.913
Weight (kg)	60.7 ± 9.2 [46.0–85.0]	64.1 ± 8.7 [48.8–85.0]	0.115
Height (cm)	155.0 ± 7.5 [140.0–170.0]	155.7 ± 5.5 [144.0–169.5]	0.666
BMI (kg/m^2)	25.3 ± 3.4 [19.6–32.8]	26.4 ± 3.3 [21.1–32.4]	0.146
Lumbar spine fracture			
Number	26	26	
Age (years)	65.8 ± 8.3 [50.0–79.7]	65.6 ± 7.6 [48.8–78.2]	0.905
Weight (kg)	60.8 ± 8.0 [46.0–75.0]	64.3 ± 9.3 [48.8–85.0]	0.151
Height (cm)	155.3 ± 8.3 [140.0–170.0]	156.4 ± 6.2 [144.0–169.5]	0.578
BMI (kg/m^2)	25.3 ± 3.2 [19.6–31.6]	26.3 ± 3.5 [21.1–32.4]	0.279
L1 vertebral fracture			
Number	15	15	
Age (years)	64.6 ± 7.7 [50.0–76.6]	64.0 ± 7.7 [48.8–75.7]	0.839
Weight (kg)	62.7 ± 7.2 [46.0–75.0]	65.6 ± 9.3 [54.5–85.0]	0.336
Height (cm)	154.3 ± 7.8 [140.0–170.0]	157.0 ± 7.6 [144.0–169.5]	0.359
BMI (kg/m^2)	26.3 ± 2.8 [21.1–31.6]	26.7 ± 3.4 [22.5–32.4]	0.780
Thoracic spine fracture			
Number	16	16	
Age (years)	63.9 ± 7.7 [50.0–74.0]	64.9 ± 8.4 [48.8–75.7]	0.738
Weight (kg)	61.7 ± 10.1 [46.0–85.0]	64.2 ± 8.2 [54.0–83.0]	0.444
Height (cm)	154.0 ± 4.7 [143.0–161.0]	156.0 ± 5.1 [148.0–169.5]	0.251
BMI (kg/m^2)	26.0 ± 3.6 [21.0–32.8]	26.4 ± 2.9 [22.0–30.8]	0.733

Results are expressed as mean ± standard deviation (minimum–maximum)

*p-values from unpaired two-sample t test

BMI, body mass index

Table 2 Vertebral fracture (whole database). DXA-derived measurements at baseline of control and fracture groups, differences between groups, AUC, and OR

L1–L4 segment	Control	Fracture	Differences	*p**	AUC	OR (95% CI)
DXA-derived 2D measurements						
aBMD	0.936 ± 0.144	0.849 ± 0.115	− 0.087 (− 9.3%)	*0.005*	0.682	2.033 [1.202–3.438][a]
BMC	47.4 ± 9.9	43.5 ± 8.1	− 3.9 (− 8.2%)	0.070	0.615	1.562 [0.957–2.550][a]
Area	50.3 ± 4.5	51.1 ± 5.4	0.8 (1.6%)	0.477	0.521	0.844 [0.531–1.341][b]
DXA-derived 3D measurements						
Integral bone, total vertebra						
Int. vBMD (total)	255.7 ± 39.6	229.7 ± 32.0	− 26.0 (− 10.2%)	*0.003*	0.687	2.158 [1.262–3.691][a]
Int. BMC (total)	41.1 ± 8.8	37.5 ± 7.1	− 3.6 (− 8.8%)	0.056	0.616	1.601 [0.979–2.619][a]
Int. volume (total)	160.6 ± 21.8	163.4 ± 20.8	2.8 (1.7%)	0.574	0.541	0.874 [0.551–1.388][b]
Integral bone, vertebral body						
Int. vBMD (body)	204.6 ± 32.8	181.4 ± 21.4	− 23.2 (− 11.3%)	< *0.001*	0.711	2.547 [1.410–4.603][a]
Int. BMC (body)	21.1 ± 4.4	19.0 ± 3.4	− 2.1 (9.8%)	*0.026*	0.636	1.757 [1.051–2.937][a]
Int. volume (body)	103.3 ± 14.8	104.8 ± 13.3	1.4 (1.4%)	0.663	0.530	0.901 [0.568–1.428][b]
Trabecular bone, vertebral body						
Trab. vBMD (body)	132.7 ± 30.2	111.3 ± 19.2	− 21.4 (− 16.1%)	< *0.001*	0.733	2.637 [1.422–4.890][a]
Trab. BMC (body)	11.9 ± 2.8	10.2 ± 2.0	− 1.7 (− 14.0%)	*0.005*	0.682	2.101 [1.217–3.627][a]
Trab. volume (body)	90.3 ± 13.5	92.1 ± 12.1	1.8 (2.0%)	0.540	0.541	0.864 [0.544–1.372][b]
Cortical bone, vertebral body						
Cort. vBMD (body)	702.4 ± 54.6	691.7 ± 62.7	− 10.7 (− 1.5%)	0.438	0.550	1.203 [0.758–1.912][a]
Cort. BMC (body)	9.2 ± 1.9	8.8 ± 1.8	− 0.4 (− 4.5%)	0.342	0.563	1.256 [0.787–2.005][a]
Cort. volume (body)	13.0 ± 1.8	12.6 ± 1.5	− 0.4 (− 3.0%)	0.317	0.577	1.272 [0.796–2.033][a]
Cort. Th. (body)	0.65 ± 0.06	0.63 ± 0.05	− 0.03 (− 4.3%)	*0.026*	0.632	1.736 [1.056–2.854][a]
Cort. sBMD (body)	51.2 ± 6.6	48.1 ± 5.0	− 3.1 (− 6.1%)	*0.026*	0.630	1.736 [1.055–2.854][a]

Measurements of control and fracture groups are expressed as mean ± standard deviation

Differences between groups are expressed as mean (percentage)

*p values from unpaired two-sample t test. p values < 0.05 are italicized

[a] Odds ratios correspond to a 1 SD decrease in the measurement

[b] Odds ratios correspond to a 1 SD increase in the measurement

AUC, area under the receiver operating curve; *OR*, odds ratio; *CI*, confidence intervals

aBMD, areal bone mineral density (g/cm^2); *BMC*, bone mineral content (g); area (cm^2); *vBMD*, volumetric bone mineral density (mg/cm^3); volume (cm^3); *Cort. Th.*, cortical thickness (mm); *sBMD*, surface bone mineral density (mg/cm^2)

Int., integral bone; *Trab.*, trabecular bone; *Cort.*, cortical bone; *total*, total vertebra; *body*, vertebral body

$p < 0.001$). Cortical vBMD at the vertebral body was 1.5% lower in the fracture group, although not significant ($p = 0.438$). Cortical sBMD of the fracture group was 6.1% lower compared with control group ($p = 0.026$). The anatomical distribution of the average differences in trabecular vBMD in the vertebral body between subjects included in the fracture and control groups is showed in Fig. 1. Differences in trabecular vBMD were found to be more pronounced near the endplates.

Trabecular vBMD at the vertebral body was the measurement associated with the highest AUC (0.733) and OR (2.637 [1.422–4.890]). Slightly lower values were found for the integral vBMD at the vertebral body (AUC of 0.711 and OR of 2.547 [1.410–4.603]). Cortical sBMD was associated with lower AUC (0.630) and OR (1.736 [1.055–2.854]). The AUC map associated with trabecular vBMD values computed at each voxel of the volumetric images of subjects included in the fracture and control groups is showed in Fig. 2. Only AUC higher than the 90th percentile (AUC > 0.720) is shown. Maximum AUC was 0.815. Trabecular vBMD measurements show the highest AUC when computed near the endplates.

Subgroup analysis

Lumbar spine fracture subgroup

The lumbar spine fracture subgroup was composed of 26 subjects having at least one lumbar vertebral fracture. Nineteen subjects had a single lumbar vertebral fracture, and 7 subjects had multiple lumbar vertebral fractures. The 26 subjects had a

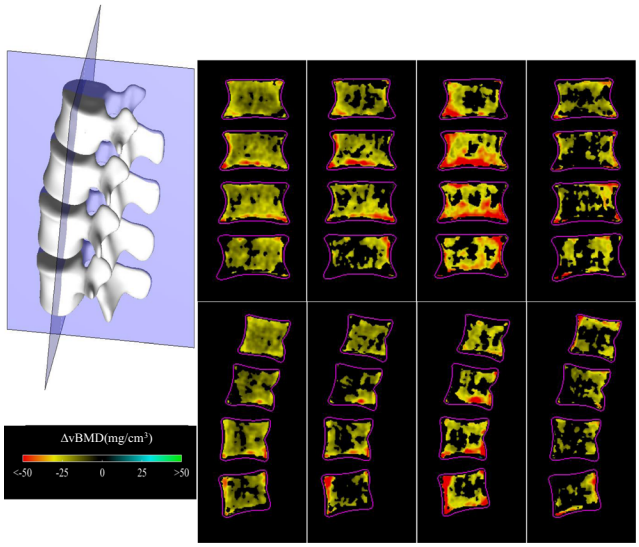

Fig. 1 Anatomical distribution of the average changes (difference between subjects included in the fracture group and subgroups and controls) in trabecular vBMD. Differences are shown in the mid-coronal plane (top) and mid-lateral plane (bottom) in the vertebral body. Top left image indicates the cut planes. Red-yellow (respectively blue-green) color indicates regions where ΔvBMD is on average lower (respectively higher) for vertebral fracture subjects compared with controls. Non-significant changes (unpaired two-sample *t* test) are left in black. The contour in pink indicates the periosteal surface of the vertebral body. Differences were computed using (from left to right) the whole database ($N = 37$ in each group), the lumbar spine fracture subgroup ($N = 26$), the L1 vertebral fracture subgroup ($N = 15$), and the thoracic spine fracture subgroup ($N = 16$)

total of 37 vertebral fractures: 2 T4, 1 T11, 5 T12, 15 L1, 6 L2, 4 L3, and 4 L4.

Mean aBMD of fracture subgroup was 10.1% lower compared with control subgroup ($p = 0.015$, Table 3). Difference in integral vBMD was − 11.2% ($p < 0.01$) at the total vertebra and − 11.8% ($p < 0.01$) at the vertebral body. Trabecular vBMD at the vertebral body of fracture subgroup was 17.8% lower compared with controls ($p < 0.01$). No significant differences were observed in measurements at the cortical bone. Trabecular vBMD was associated with the highest AUC (0.720) and OR (2.487 [1.242–4.979]). General and local findings for the lumbar spine fracture subgroup were similar to those obtained with the analysis of the whole database (Tables 2 and 3; Figs. 1 and 2). The 90th percentile threshold and the maximum value at the trabecular vBMD AUC map were 0.712 and 0.812, respectively (Fig. 2).

L1 vertebral fracture subgroup

The L1 vertebral fracture subgroup was composed of 15 subjects having at least a L1 fracture. Nine subjects had only a L1 fracture and 6 subjects had multiple vertebral fractures. The 15 subjects had a total of 24 vertebral fractures: 2 T4, 1 T11, 5 T12, 15 L1, and 2 L2.

More pronounced differences were observed in this subgroup (Table 3), especially when looking at the trabecular vBMD in the vertebral body (− 23.7%, $p < 0.01$). No significant differences were observed in measurements at the cortical bone. Trabecular vBMD in the vertebral body was the measurement associated with the highest AUC (0.827) and OR (5.043 [1.448–17.556]). Differences in trabecular vBMD were locally more pronounced (Fig. 1) and associated with higher AUC (Fig. 2), compared with values found when analyzing the whole database.

Thoracic spine fracture subgroup

The thoracic spine fracture subgroup was composed of 16 subjects having at least one thoracic vertebral fracture. Eleven subjects had a single thoracic vertebral fracture and 5 subjects had multiple vertebral fractures. The 16 subjects had a total of 25 vertebral fractures: 2 T4, 2 T7, 1 T8, 1 T9, 3 T10, 1 T11, 9 T12, 5 L1, and 1 L2.

No significant differences were observed in aBMD and cortical vBMD between the thoracic spine fracture subgroup and control subgroup (Table 3). In the vertebral body, differences in vBMD were more pronounced in the trabecular bone (− 16.2%, $p < 0.01$), than in the integral bone (− 12.8%, $p < 0.01$).

Trabecular vBMD was associated with the highest AUC (0.801) and OR (5.060 [1.406–18.208]) compared with the other DXA-derived measurements. Differences in trabecular vBMD were locally less pronounced in the thoracic spine fracture subgroup, compared with the L1 vertebral fracture subgroup (Fig. 1). However, trabecular vBMD values were locally associated with higher AUC, compared with values found when analyzing the whole database (Fig. 2).

Unlike the other subgroups analyses, significant differences ($p = 0.018$) were observed in cortical sBMD between the thoracic spine fracture subgroup and controls. Cortical sBMD was associated with higher AUC (0.734) and OR (2.649 [1.111–6.313]), compared with other measurements at the cortex. The anatomical distribution of the average differences in cortical sBMD between subjects included in thoracic spine fracture analysis and controls is showed in Fig. 3 (top). More pronounced differences (magenta color) were found at the endplates of vertebrae L1, L2, and L4. Figure 3 also shows the AUC calculated using cortical sBMD at each vertex of the vertebral body surface. AUC higher than the 90th percentile (i.e., in the range 0.777–0.836) is circled in red and were mostly found at the endplates.

Discussion

In the present study, the ability of DXA-derived 3D measurements at lumbar spine to discriminate between

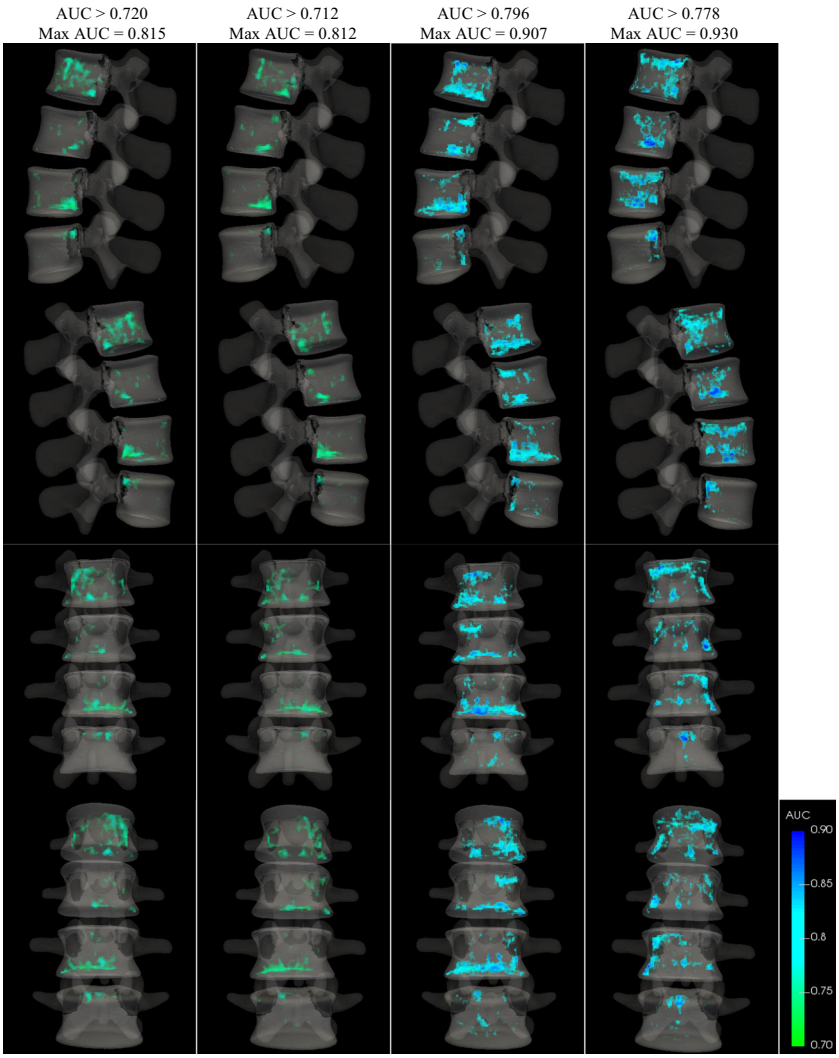

Fig. 2 AUC map calculated using trabecular vBMD at each voxel of the volumetric images of subjects included in the fracture group and controls. Only AUC higher than the 90th percentile is shown. Differences were computed using (from left to right) the whole database ($N = 37$ in each group), the lumbar spine fracture subgroup ($N = 26$), the L1 vertebral fracture subgroup ($N = 15$), and the thoracic spine fracture subgroup ($N = 16$)

postmenopausal women with and without osteoporosis-related vertebral fractures was evaluated. The DXA-derived 3D measurements were performed at baseline (at least 1 year before the vertebral fracture event), using standard DXA scans and a 3D modeling technique [27]. To the best of our knowledge, no retrospective case-control study evaluating the association of DXA-derived 3D measurements at vertebrae L1 to L4 with osteoporosis-related vertebral fractures has been reported in the literature.

Age, sex, and BMI are independent risk factors for osteoporosis-related fractures [5, 6]. In the present study, an age-matched database of postmenopausal women was used, in order to eliminate the confounding effect of age and sex. Although no inclusion criteria related to height or weight was used to recruit the subjects, no significant differences between groups were found in terms of height, weight, and BMI at baseline (Table 1).

Significant differences between fracture and control groups were observed for aBMD (− 9.3%, $p < 0.01$), integral vBMD (− 10.2%, $p < 0.01$), and trabecular vBMD (− 16.1%, $p < 0.001$, Table 2). We found slightly higher OR for DXA-derived vBMD measurements in the vertebral body (2.547 [1.410–4.603] at the integral bone and 2.637 [1.422–4.890] at the trabecular bone, Table 2) compared with aBMD (2.033 [1.202–3.438]). This is consistent with the literature, where OR for QCT-based vBMD measurements was found to be similar or higher, compared with aBMD measurements [16–18]. Melton et al. [16] reported slightly higher OR for vBMD at L1–L3 segment (2.2 [1.1–4.3] at the integral bone and 1.9 [1.0–3.6] at the trabecular bone), compared with aBMD (0.7 [0.4–1.2]). Anderson et al. [17] reported higher OR for vBMD at L3 (3.4 [1.7–6.8] at the integral bone and 3.4 [1.7–6.9] at the trabecular bone), compared with aBMD (1.9 [1.1–3.3]). Grampp et al. [18] reported higher OR for vBMD at L1–L4 segment (3.0 [1.5–6.1] at the integral bone and 4.3 [1.8–10.1] at the trabecular bone), compared with aBMD (2.4 [1.4–4.2]).

Trabecular vBMD at the vertebral body was the measurement that best discriminates between fracture and control groups, with an AUC of 0.733, against 0.682 for aBMD (Table 2). Similar findings were reported in QCT-based

Table 3 Subgroups analysis according to fracture site. DXA-derived measurements at baseline of subjects included in the control and fracture groups, differences between groups, AUC, and OR

L1–L4 segment	Control	Fracture	Differences	*p**	AUC	OR (95% CI)
Lumbar spine fracture						
aBMD	0.945 ± 0.159	0.850 ± 0.110	− 0.095 (− 10.1%)	*0.015*	0.686	2.109 [1.117–3.982][a]
Int. vBMD (total)	258.9 ± 44.1	230.0 ± 32.1	− 28.9 (− 11.2%)	*0.009*	0.692	2.226 [1.172–4.226][a]
Int. vBMD (body)	206.0 ± 37.8	181.6 ± 22.9	− 24.4 (− 11.8%)	*0.007*	0.695	2.348 [1.202–4.589][a]
Trab. vBMD (body)	134.3 ± 35.1	110.4 ± 21.6	− 23.9 (− 17.8%)	*0.005*	0.720	2.487 [1.242–4.979][a]
Cort. vBMD (body)	700.4 ± 55.0	699.7 ± 53.8	− 0.7 (− 0.1%)	0.963	0.501	1.013 [0.585–1.754][a]
Cort. Th. (body)	0.66 ± 0.07	0.63 ± 0.05	− 0.03 (− 4.0%)	0.100	0.608	1.623 [0.907–2.906][a]
Cort. sBMD (body)	51.5 ± 7.3	48.6 ± 5.1	− 2.9 (− 5.7%)	0.099	0.608	1.625 [0.908–2.910][a]
L1 vertebral fracture						
aBMD	0.982 ± 0.147	0.868 ± 0.115	− 0.114 (− 11.6%)	*0.025*	0.758	2.557 [1.068–6.125][a]
Int. vBMD (total)	272.9 ± 38.5	236.6 ± 33.6	− 36.3 (− 13.3%)	*0.010*	0.747	3.058 [1.186–7.886][a]
Int. vBMD (body)	220.7 ± 33.4	186.5 ± 23.6	− 34.2 (− 15.5%)	*0.003*	0.778	4.013 [1.354–11.894][a]
Trab. vBMD (body)	147.9 ± 30.8	112.8 ± 22.5	− 35.1 (− 23.7%)	*0.001*	0.827	5.043 [1.448–17.556][a]
Cort. vBMD (body)	705.6 ± 60.8	718.1 ± 54.5	12.6 (1.8%)	0.556	0.551	0.795 [0.380–1.661][b]
Cort. Th. (body)	0.67 ± 0.07	0.64 ± 0.05	− 0.03 (− 4.7%)	0.159	0.640	1.757 [0.803–3.846][a]
Cort. sBMD (body)	53.1 ± 7.4	49.5 ± 5.7	− 3.5 (− 6.6%)	0.158	0.644	1.761 [0.804–3.856][a]
Thoracic spine fracture						
aBMD	0.931 ± 0.126	0.856 ± 0.133	− 0.076 (− 8.1%)	0.110	0.662	1.862 [0.862–4.022][a]
Int. vBMD (total)	256.2 ± 36.6	230.0 ± 34.0	− 26.2 (− 10.2%)	*0.044*	0.691	2.296 [0.974–5.413][a]
Int. vBMD (body)	207.6 ± 24.1	181.0 ± 20.5	− 26.6 (− 12.8%)	*0.002*	0.793	4.557 [1.411–14.718][a]
Trab. vBMD (body)	134.5 ± 21.2	112.7 ± 16.3	− 21.8 (− 16.2%)	*0.003*	0.801	5.060 [1.406–18.208][a]
Cort. vBMD (body)	704.3 ± 47.9	687.9 ± 77.2	− 16.3 (− 2.3%)	0.477	0.543	1.307 [0.639–2.673][a]
Cort. Th. (body)	0.66 ± 0.06	0.62 ± 0.05	− 0.05 (− 7.1%)	*0.017*	0.734	2.659 [1.115–6.342][a]
Cort. sBMD (body)	52.2 ± 6.5	47.0 ± 5.1	− 5.2 (− 10.0%)	*0.018*	0.734	2.649 [1.111–6.313][a]

Results are given for the subgroups analysis: lumbar spine fracture, L1 vertebral fracture, and thoracic spine fracture

Measurements of control and fracture groups are expressed as mean ± standard deviation

Differences between groups are expressed as mean (percentage)

*p values from unpaired two-sample t test. p values < 0.05 are italicized

[a] Odds ratios correspond to a 1 SD decrease in the measurement

[b] Odds ratios correspond to a 1 SD increase in the measurement

AUC, area under the receiver operating curve; *OR*, odds ratio; *CI*, confidence intervals

aBMD, areal bone mineral density (g/cm^2); *vBMD*, volumetric bone mineral density (mg/cm^3); *Cort. Th.*, cortical thickness (mm); *sBMD*, surface bone mineral density (mg/cm^2)

Int., integral bone; *Trab.*, trabecular bone; *Cort.*, cortical bone; *total*, total vertebra; *body*, vertebral body

studies in the literature. Chalhoub et al. [15] reported an AUC of 0.79 for trabecular vBMD, against 0.72 for aBMD. Melton et al. [16] reported an AUC of 0.78 for trabecular vBMD, against 0.75 for aBMD. Grampp et al. [18] reported an AUC of 0.82 for trabecular vBMD, against 0.78 for aBMD. Imai et al. [22] reported an AUC of 0.77 for trabecular vBMD, against 0.71 for aBMD.

The use of QCT-based vBMD measurements to overcome limitations related to aBMD measurements has been proposed by several studies in the literature [5, 6, 13–19, 29]. DXA-derived 3D measurements have the potential to provide similar output measurements, but without the disadvantages of QCT (high financial cost and radiation dose, compared with DXA) [23–27].

Spinal degeneration, abdominal aortic calcification, and other sclerotic lesions artificially increase aBMD as measured by DXA [5, 6, 13, 29], although patients with such pathologies have higher fracture risk. DXA-derived measurement of the trabecular vBMD in the vertebral body could be less sensitive to artifacts produced by those diseases that are often located at the vertebral surface (cortical bone) or in the posterior arch. This could explain the higher AUC values found for trabecular vBMD measurements found in our study. In this sense, DXA-derived 3D measurements of the trabecular bone at the vertebral body could provide an alternative measurement, overcoming the limitation of aBMD-based diagnosis by discarding bone

spurs, local deformations at the periosteal surface, or in the back processes [29].

In the present study, differences were less pronounced in the cortical bone (cortical sBMD − 6.1%, AUC = 0.630) than in the trabecular bone (trabecular vBMD − 16.1%, AUC = 0.733, Table 2). Studies using biomechanical testing showed that the contribution of the cortical bone to vertebral strength is usually low in normal subjects, but it could be important in older osteoporotic subjects [30, 31]. Accuracy of the DXA-derived measurements in the trabecular and cortical bone was assessed in previous work [27]. However, the cortex of the vertebral body is very thin (from 180 to 600 μm with a mean thickness of 380 μm [32]), and the DXA-based 3D modeling methods can hardly model local deformities, which could affect the accuracy of cortical bone measurements. The cortical sBMD is considered a more robust measurement of the cortical bone than cortical vBMD or Th, since it is, in general, easier to measure in low-resolution images [33, 34].

The fracture group included in this study included various types of vertebral fractures. Subgroup analyses assessing differences between groups depending on the type of fracture were also performed. The type of vertebral fractures found in the 37 cases included in this study was consistent with the literature, with a higher prevalence around the thoracolumbar junction (T12–L1) [17, 35]. Although the reason for this higher prevalence remains unknown, it has been suggested that thoracic kyphosis and the stiffness of the rib cage predispose this area to fracture by increasing vertebral loading in this location.

Overall, similar findings were observed within the subgroups analyses (Table 3): significant differences for integral and trabecular vBMD and no significant differences for cortical vBMD. Trabecular vBMD at the vertebral body was also the measurement that best discriminates between fracture and control subgroups. Interestingly, differences between fractured subject and controls were found to be more pronounced when analyzing the L1 vertebral fracture subgroup (trabecular vBMD − 23.7%), than when assessing the whole database (− 16.1%). This can be explained by the fact that measurements were performed at the L1–L4 segment, which includes the vertebra that will fracture in all subjects of the L1 vertebral fracture subgroup. This is consistent with the literature, where site-specific measurements showed higher accuracy to discriminate osteoporosis-related fractures than other sites measurements [5–7].

Although site-specific measurements showed higher accuracy, the overlying ribcage prevents the use of DXA to determine BMD in the thoracic spine. Therefore, on the third subgroup analysis, we assessed the association of DXA-derived 3D measurements at the lumbar spine with thoracic spine fractures. Interestingly, no significant differences were observed in aBMD ($p = 0.110$), whereas significant differences were observed in trabecular vBMD at the vertebral body ($p < 0.01$). Budoff et al. [36] found a high correlation between trabecular vBMD measured at the lumbar vertebrae and trabecular vBMD at thoracic vertebrae. We found higher OR and AUC for trabecular vBMD (OR = 5.060 [1.411–18.208], AUC = 0.801), compared with aBMD (OR = 1.862 [0.862–

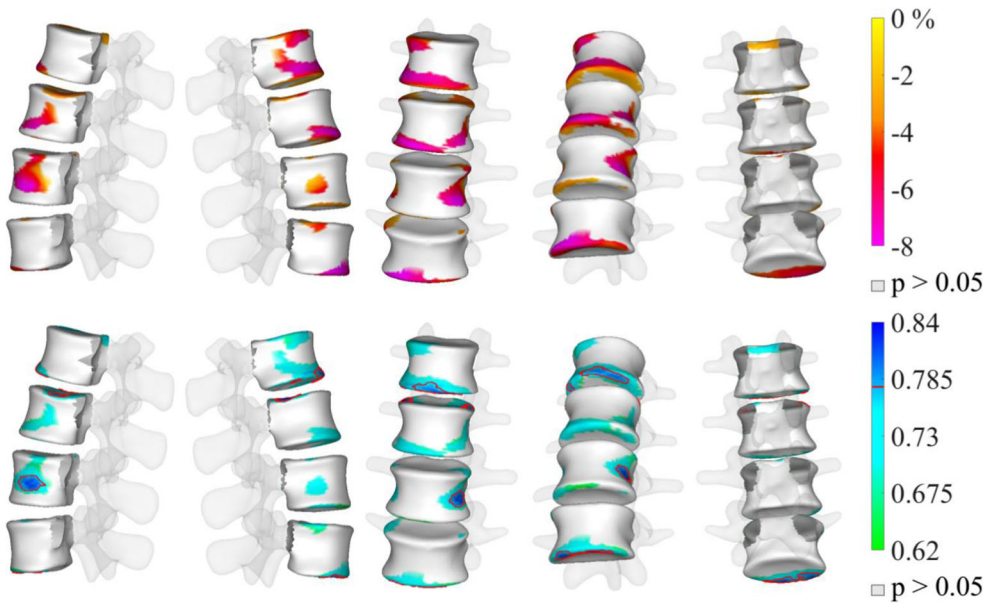

Fig. 3 Top: anatomical distribution of the average differences in cortical sBMD at the vertebral body between subjects included in the thoracic spine fracture subgroup ($N = 16$) and its respective controls ($N = 16$). Non-significant changes (unpaired two-sample t test) are left in gray. Bottom: AUC calculated using cortical sBMD at each vertex of the vertebral body surface of the subjects included in thoracic spine fracture and control groups. Regions where the differences in cortical sBMD were not significant (unpaired two-sample t test) at the total vertebra region of interest are left in gray. Regions showing AUC higher than the 90th percentile (i.e., AUC > 0.777) are circled in red. Maximum AUC was 0.836

4.022], AUC = 0.662). Anderson et al. [17] reported higher OR for vBMD at L3 (5.3 [1.3–21] at the integral bone and 5.6 [1.3–23.4] at the trabecular bone), compared with aBMD (2.8 [1.0–8.0]).

Local differences between fracture and control groups were analyzed using color-coded images (Fig. 1, 2, and 3). Average differences in trabecular vBMD between subjects included in fracture groups and controls (Fig. 1) and associated AUC (Fig. 2) were higher near the endplates and lower in the center of the vertebral body. The endplates are the regions where tissue-level failure started, as measured in specimens with experimentally observed vertebral fracture [30, 37–39]. Those findings are consistent with biomechanical testing studies that show the maximum load fraction in the trabecular bone typically occurring near the endplates [22, 30, 39]. Anatomical distribution of differences in trabecular vBMD between subjects included in fracture and control groups was more uniform at the whole database than in the subgroups, and the highest difference was found in the L1 vertebral fracture subgroup (Fig. 1). The L1 vertebral fracture and the thoracic spine fracture subgroups showed the highest AUCs, with maximum values of 0.907 and 0.930, respectively (Fig. 2). The anatomical distribution of the average differences in cortical sBMD between subjects included in thoracic spine fracture subgroup and its respective control subgroup shows more pronounced differences at the endplates (Fig. 3) [30, 37–39]. Results showed in Figs. 1, 2, and 3 were consistent with state-of-the-art studies using biomedical testing that show endplate thickness and density and adjacent trabecular bone density as good predictors of local stiffness and strength.

The most important limitation of our study is the small number of subjects included. The main difficulties in including subjects in the fracture group were to find patients with DXA images before the incident fracture, as most of patients go to the medical office after the fracture event, and to make sure that the subjects had no prevalent osteoporosis-related fracture at any skeletal site at baseline. Besides, our study is monocentric, which only includes postmenopausal Caucasian women and not all of them have the same vertebra fractured. Therefore, results can be only extrapolated to populations with similar characteristics. Also, due to the design of our study (retrospective and case-control), we cannot directly imply a causative association between reduced DXA-derived 3D measurements and osteoporosis-related fracture. Another limitation is that participants included in this study did not undergo QCT examination. Therefore, we could not perform a direct comparison between the results obtained using DXA-derived 3D measurements with QCT-derived measurements. Moreover, the presence/absence of vertebral fracture was confirmed using anteroposterior DXA scans and VFA. It would have been interesting to include other imaging modalities such as QCT or X-rays to further assess vertebral fractures.

Conclusions

This case-control study showed the association of DXA-derived 3D measurements at the lumbar spine with osteoporosis-related vertebral fractures. Lower vBMD at different vertebral regions and bone compartments was found in fracture group and subgroups compared with controls. Trabecular vBMD at the vertebral body was the measurement that best discriminates between fracture and control groups. DXA-based 3D modeling approaches could be a valuable option to complement standard DXA-derived 2D measurements in osteoporosis management. Similar studies including large cohorts will be performed in future work to determine if DXA-derived 3D measurements at the lumbar spine could improve fracture risk prediction in clinical practice.

Funding information We would like to acknowledge the support from the Industrial Doctorates program of the *Generalitat de Catalunya*, as well as the QUAES Foundation - UPF Chair for Computational Tools for Healthcare. The research leading to these results has also received funding from *Programa Estatal de Investigación, Desarrollo e Innovación Orientada a los Retos de la Sociedad*, *Ministerio de Economía y Competitividad* (Reference: RTC-2014-2740-1) and Eurostars program (Project ID: 9 140) funded by *Centro para el Desarrollo Tecnológico Industrial, Ministerio de Economía Competitividad.*

Compliance with ethical standards

Conflicts of interest M. López Picazo is an employee of Galgo Medical. L. Humbert is a stockholder and employee of Galgo Medical. S. Di Gregorio, M. A. González Ballester and L. Del Rio have no conflict of interest.

References

1. Johnell O, Kanis JA (2006) An estimate of the worldwide prevalence and disability associated with osteoporotic fractures. Osteoporos Int 17:1726–1733. https://doi.org/10.1007/s00198-006-0172-4
2. Ballane G, Cauley JA, Luckey MM, El-Hajj Fuleihan G (2017) Worldwide prevalence and incidence of osteoporotic vertebral fractures. Osteoporos Int 28:1531–1542. https://doi.org/10.1007/s00198-017-3909-3
3. Cummings SR, Melton LJ (2002) Epidemiology and outcomes of osteoporotic fractures. Lancet 359:1761–1767. https://doi.org/10.1016/S0140-6736(02)08657-9
4. Jalava T, Sarna S, Pylkka L et al (2003) Association between vertebral fracture and increased mortality in osteoporotic patients. J Bone Miner Res 18:1254–1259
5. Kanis JA (2002) Diagnosis of osteoporosis and assessment of fracture risk. Lancet 359:1929–1936. https://doi.org/10.1016/S0140-6736(02)08761-5
6. Kanis JA, Johansson H, Oden A, McCloskey EV (2009) Assessment of fracture risk. Eur J Radiol 71:392–397. https://doi.org/10.1016/j.ejrad.2008.04.061

7. Marshall D, Wedel H (1996) Meta-analysis of how well measures of bone mineral density predict occurrence of osteoporotic fractures. BMJ 312:1254–1259. https://doi.org/10.1136/bmj.312.7041.1254
8. Siris ES, Chen Y-T, Abbott TA, Barrett-Connor E, Miller PD, Wehren LE, Berger ML (2004) Bone mineral density thresholds for pharmacological intervention to prevent fractures. Arch Intern Med 164:1108–1112. https://doi.org/10.1001/archinte.164.10.1108
9. Dimai HP (2017) Use of dual-energy X-ray absorptiometry (DXA) for diagnosis and fracture risk assessment; WHO-criteria, T- and Z-score, and reference databases. Bone 104:39–43. https://doi.org/10.1016/j.bone.2016.12.016
10. Gordon CM, Lang TF, Augat P, Genant HK (1998) Image-based assessment of spinal trabecular bone structure from high-resolution CT images. Osteoporos Int 8:317–325. https://doi.org/10.1007/s001980050070
11. Genant HK, Wu CY, van Kuijk C, Nevitt MC (1993) Vertebral fracture assessment using a semiquantitative technique. J Bone Miner Res 8:1137–1148. https://doi.org/10.1002/jbmr.5650080915
12. Prevrhal S, Fox JC, Shepherd JA, Genant HK (2003) Accuracy of CT-based thickness measurement of thin structures : modeling of limited spatial resolution in all three dimensions. Med Phys 30:1–8. https://doi.org/10.1118/1.1521940
13. Li N, Li XM, Xu L, Sun WJ, Cheng XG, Tian W (2013) Comparison of QCT and DXA: osteoporosis detection rates in postmenopausal women. Int J Endocrinol 2013:1–5. https://doi.org/10.1155/2013/895474
14. Engelke K, Libanati C, Fuerst T, Zysset P, Genant HK (2013) Advanced CT based in vivo methods for the assessment of bone density, structure, and strength. Curr Osteoporos Rep 11:246–255. https://doi.org/10.1007/s11914-013-0147-2
15. Chalhoub D, Orwoll ES, Cawthon PM, Ensrud KE, Boudreau R, Greenspan S, Newman AB, Zmuda J, Bauer D, Cummings S, Cauley JA, Osteoporotic Fractures in Men (MrOS) Study Research Group (2016) Areal and volumetric bone mineral density and risk of multiple types of fracture in older men. Bone 92:100–106. https://doi.org/10.1016/j.bone.2016.08.014
16. Melton LJ, Riggs BL, Keaveny TM et al (2007) Structural determinants of vertebral fracture risk. J Bone Miner Res 22:1885–1892. https://doi.org/10.1359/jbmr.070728
17. Anderson DE, Demissie S, Allaire BT, Bruno AG, Kopperdahl DL, Keaveny TM, Kiel DP, Bouxsein ML (2014) The associations between QCT-based vertebral bone measurements and prevalent vertebral fractures depend on the spinal locations of both bone measurement and fracture. Osteoporos Int 25:559–566. https://doi.org/10.1111/j.1743-6109.2008.01122.x.Endothelial
18. Grampp S, Genant HK, Mathur A, Lang P, Jergas M, Takada M, Glüer CC, Lu Y, Chavez M (1997) Comparisons of noninvasive bone mineral measurements in assessing age- related loss, fracture discrimination, and diagnostic classification. J Bone Miner Res 12:697–711. https://doi.org/10.1359/jbmr.1997.12.5.697
19. Kopperdahl DL, Aspelund T, Hoffmann PF, Sigurdsson S, Siggeirsdottir K, Harris TB, Gudnason V, Keaveny TM (2014) Assessment of incident spine and hip fractures in women and men using finite element analysis of CT scans. J Bone Miner Res 29:570–580. https://doi.org/10.1002/jbmr.2069.Assessment
20. Wang X, Sanyal A, Cawthon P et al (2012) Prediction of new clinical vertebral fractures in elderly men using FEA of CT scans. J Bone Miner Res 27:808–816. https://doi.org/10.1002/jbmr.1539.Prediction
21. Zysset P, Qin L, Lang T, Khosla S, Leslie WD, Shepherd JA, Schousboe JT, Engelke K (2015) Clinical use of quantitative computed tomography–based finite element analysis of the hip and spine in the management of osteoporosis in adults: the 2015 ISCD official positions—part II. J Clin Densitom 18:359–392. https://doi.org/10.1016/j.jocd.2015.06.011
22. Imai K, Ohnishi I, Matsumoto T, Yamamoto S, Nakamura K (2009) Assessment of vertebral fracture risk and therapeutic effects of alendronate in postmenopausal women using a quantitative computed tomography-based nonlinear finite element method. Osteoporos Int 20:801–810. https://doi.org/10.1007/s00198-008-0750-8
23. Ahmad O, Ramamurthi K, Wilson KE, Engelke K, Prince RL, Taylor RH (2010) Volumetric DXA (VXA): a new method to extract 3D information from multiple in vivo DXA images. J Bone Miner Res 25:2744–2751. https://doi.org/10.1002/jbmr.140
24. Väänänen SP, Grassi L, Flivik G, Jurvelin JS, Isaksson H (2015) Generation of 3D shape, density, cortical thickness and finite element mesh of proximal femur from a DXA image. Med Image Anal 24:125–134. https://doi.org/10.1016/j.media.2015.06.001
25. Humbert L, Martelli Y, Fonolla R, Steghofer M, di Gregorio S, Malouf J, Romera J, Barquero LMDR (2017) 3D-DXA: assessing the femoral shape, the trabecular macrostructure and the cortex in 3D from DXA images. IEEE Trans Med Imaging 36:27–39. https://doi.org/10.1109/TMI.2016.2593346
26. Whitmarsh T, Humbert L, Del Río Barquero LM et al (2013) 3D reconstruction of the lumbar vertebrae from anteroposterior and lateral dual-energy X-ray absorptiometry. Med Image Anal 17:475–487. https://doi.org/10.1016/j.media.2013.02.002
27. López Picazo M, Magallón Baro A, del Rio Barquero LM et al (2018) 3D subject-specific shape and density estimation of the lumbar spine from a single anteroposterior DXA image including assessment of cortical and trabecular bone. IEEE Trans Med Imaging 37:2651–2662. https://doi.org/10.1109/TMI.2018.2845909
28. Humbert L, Hazrati Marangalou J, Del Río Barquero LM et al (2016) Technical note: cortical thickness and density estimation from clinical CT using a prior thickness-density relationship. Med Phys 43:1945–1954. https://doi.org/10.1118/1.4944501
29. Guglielmi G, Floriani I, Torri V, Li J, van Kuijk C, Genant HK, Lang TF (2005) Effect of spinal degenerative changes on volumetric bone mineral density of the central skeleton as measured by quantitative computed tomography. Acta Radiol 46:269–275. https://doi.org/10.1080/02841850510012661
30. Eswaran SK, Gupta A, Adams MF, Keaveny TM (2006) Cortical and trabecular load sharing in the human vertebral body. J Bone Miner Res 21:307–314. https://doi.org/10.1359/JBMR.051027
31. Roux JP, Wegrzyn J, Arlot ME, Guyen O, Delmas PD, Chapurlat R, Bouxsein ML (2010) Contribution of trabecular and cortical components to biomechanical behavior of human vertebrae: an ex vivo study. J Bone Miner Res 25:356–361. https://doi.org/10.1359/jbmr.090803
32. Chen H, Zhou X, Fujita H, Onozuka M, Kubo KY (2013) Age-related changes in trabecular and cortical bone microstructure. Int J Endocrinol 2013:1–9. https://doi.org/10.1155/2013/213234
33. Treece GM, Gee AH (2015) Independent measurement of femoral cortical thickness and cortical bone density using clinical CT. Med Image Anal 20:249–264. https://doi.org/10.1016/j.media.2014.11.012
34. Winzenrieth R, Humbert L, Di Gregorio S et al (2018) Effects of osteoporosis drug treatments on cortical and trabecular bone in the femur using DXA-based 3D modeling. Osteoporos Int 29:2323–2333
35. Van der Klift M, De Laet CE, McCloskey EV et al (2002) The incidence of vertebral fractures in men and women: the Rotterdam Study. J Bone Miner Res 17:1051–1056
36. Budoff MJJ, Khairallah W, Li D et al (2012) Trabecular bone mineral density measurement using thoracic and lumbar quantitative computed tomography. Acad Radiol 19:179–183. https://doi.org/10.1016/j.acra.2011.10.006
37. Noshchenko A, Plaseied A, Patel V et al (2013) Correlation of vertebral strength topography with 3-dimensional computed tomographic structure. Spine (Phila Pa 1976) 38:339–349

38. Jackman TM, Hussein AI, Adams AM, Makhnejia KK, Morgan EF (2014) Endplate deflection is a defining feature of vertebral fracture and is associated with properties of the underlying trabecular bone. J Orthop Res 32:880–886. https://doi.org/10.1002/jor.22620

39. Jackman TM, Hussein AI, Curtiss C, Fein PM, Camp A, de Barros L, Morgan EF (2016) Quantitative, 3D visualization of the initiation and progression of vertebral fractures under compression and anterior flexion. J Bone Miner Metab 31:777–788. https://doi.org/10.1002/jbmr.2749